

# PERMANENT MAGNETS FOR ACCELERATORS

B. J. A. Shepherd<sup>†,1</sup>, STFC Daresbury Laboratory, Warrington WA4 4AD, UK  
<sup>1</sup>also at Cockcroft Institute, Warrington WA4 4AD, UK

## Abstract

Several groups internationally have been designing and building adjustable permanent magnet based quadrupoles for light sources, colliders, and plasma accelerators because of their very high gradients and zero power consumption. There are now examples of widely adjustable PM dipoles too. The ZEPTO project, based at STFC Daresbury Laboratory, developed several highly adjustable PM-based dipole and quadrupole prototypes for CLIC, and is now building a quadrupole to be installed in Diamond to gain experience ahead of the Diamond-2 upgrade. This is a review and comparison of the recent designs globally with comments on the future prospects.

## INTRODUCTION

Permanent magnets (PMs), are materials that retain a strong remanent magnetisation after the applied magnetising field is removed. Energy is stored in the material, and a PM can produce a strong field especially when combined with other ferromagnetic elements to form a flux circuit.

Development of PMs is arguably one of the technological success stories of the 20<sup>th</sup> century [1], with the energy product  $BH_{max}$  doubling on average every twelve years thanks to the discovery of ferrites and later SmCo and NdFeB (Fig. 1), the latter being an ‘almost ideal’ PM material with a high proportion of iron and a relatively abundant rare-earth element. Both  $\text{Sm}_2\text{Co}_{17}$  and  $\text{Nd}_2\text{Fe}_{14}\text{B}$  are near their theoretical maxima of 294 kJ/m<sup>3</sup> and 512 kJ/m<sup>3</sup> respectively. The discovery of new PMs led to technological developments in many other fields, including information storage, transport and energy generation.

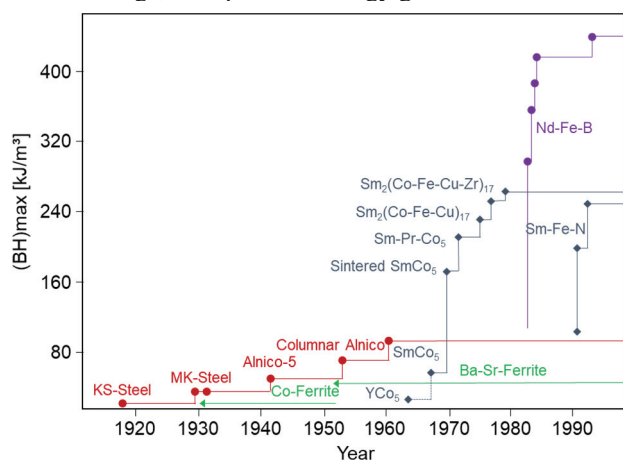


Figure 1: Development of PMs in the 20<sup>th</sup> century.

In accelerators, a major use of PMs over the years has been undulators and wigglers (insertion devices or IDs) in light sources [2], first proposed by Ginzburg in 1947 and

used in storage rings from the 1970s onwards. When short periods and small gaps are required, PMs are usually a better choice for IDs. The Halbach array with four magnets per period gives an enhanced field on one side of each array which combines to give a strong field in the beam tube. These IDs have been extensively written about elsewhere [3] and are not the focus of this paper.

## BEAMLINE PM DEVICES

The Halbach array can also be ‘wrapped’ around a cylinder to create a multipole magnet [4, 5]. Fields from an array of wedge-shaped PMs combine to give a strong field in the magnet centre (Fig. 2). These magnets typically have small apertures, and high gradients can be achieved. The gradient in a Halbach quadrupole is given by:

$$G = 2B_r K \left( \frac{1}{r_i} - \frac{1}{r_e} \right)$$

Here,  $B_r$  is the remanent field in the PM,  $r_i$  and  $r_e$  are the inner and outer radii, and  $K$  is an efficiency factor which approaches 1 as the number of segments increases.

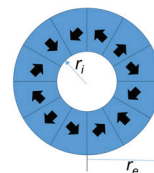


Figure 2: Schematic of a Halbach PM quadrupole, showing the inner and outer radii of the PMs.

Other multipole magnets (e.g. dipoles, sextupoles and combined function magnets) can be produced in this way.

Light source upgrades in recent years have focused on increasing the brightness, which often means a push to smaller apertures. When an electromagnet is scaled down by a factor  $k$ , if the current density is kept equal, the field will be reduced by  $k$ . In order to restore the field, either the current density or cross-section of the coils must be increased. PM-based magnets do not have this limitation, and this seems to favour the use of PM magnets for lower-aperture devices [6].

## Advantages of Permanent Magnets

PM-based magnets require no current to provide a constant field. No large power supplies are required, and no current-carrying cables. No heat is dissipated, and so no water cooling is required (which also eliminates a potential source of vibration). So overall the infrastructure and running costs can be lower than electromagnets, and of course the CO<sub>2</sub> emissions during operation are greatly reduced.

<sup>†</sup> ben.shepherd@stfc.ac.uk

# THE FUTURE CIRCULAR COLLIDER STUDY\*

A.-S. Müller, Karlsruhe Institute of Technology (KIT), 76131 Karlsruhe, Germany  
M. Benedikt, F. Zimmermann†, CERN, 1211 Geneva 23, Switzerland

## Abstract

At the end of 2018, a large worldwide collaboration, with contributors from more than 350 institutes completed the conceptual design of the Future Circular Collider (FCC), a  $\sim 100$  km accelerator infrastructure linked to the existing CERN complex, that would open up the way to the post-LHC era in particle physics. We present an overview of the two main accelerator options considered in the design study, namely the lepton collider (FCC-ee), serving as highest-luminosity Higgs and electroweak factory, and the 100-TeV energy-frontier hadron collider (FCC-hh), along with the ongoing technological R&D efforts and the planned next steps. A recently approved EU co-funded project, the FCC Innovation Study (FCCIS), will refine the design of the lepton collider and prepare the actual implementation of the FCC, in collaboration with European and global partners, and with the local authorities.

## INTRODUCTION

The FCC Conceptual Design Report (CDR) [1–4] was released at the end of 2018. The results of the conceptual design study naturally gave rise to an integrated FCC programme [5–7], which was proposed as input to the European Strategy Process: Inspired by the successful past LEP-LHC sequence at CERN, this integrated programme features in its first stage the lepton collider FCC-ee — namely a Higgs and electroweak factory, which will produce  $Z$ ,  $W$  and  $H$  bosons, and top quarks at considerable rates: At its design luminosity, FCC-ee will repeat the the entire LEP  $Z$  physics programme in about 1 minute. The second stage will be the FCC-hh proton collider ( $\sim 100$  TeV c.m. energy) as the natural continuation of the LHC at the energy frontier, with additional ion and lepton-hadron collision options. The integrated FCC programme represents a comprehensive cost-effective approach, aimed at maximizing the physics opportunities. FCC-ee and hh will offer complementary physics, while profiting from common civil engineering and technical infrastructures. They will both build on, and reuse, CERN’s existing infrastructure. In addition, the FCC integrated project, with its technical schedule, allows for a seamless continuation of High Energy Physics (HEP) after the High Luminosity LHC (HL-LHC) programme, expected to end in the second half of the 2030’s.

\* This work was supported, in part, by the European Commission under the HORIZON2020 Research and Innovation Programme, grant agreement 951754 (FCCIS).

† frank.zimmermann@cern.ch

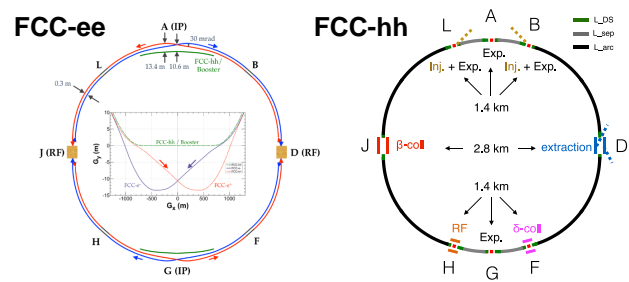


Figure 1: Layouts of FCC-ee and FCC-hh successively housed in the same tunnel [2, 3, 6].

## FCC-ee

FCC-ee is conceived as a double-ring  $e^+e^-$  collider whose 97.75 km baseline circumference follows the footprint of FCC-hh, except around the Interaction Points (IPs) at locations A and G — see Fig. 1. The FCC Interaction Region (IR) features an asymmetric layout and optics in order to limit synchrotron radiation (SR) emitted towards the detector [8]. The critical photon energy is kept below 100 keV over the last 450 m from the IP, which is one of the lessons learnt from the LEP collider [9]. The present baseline envisions 2 IPs. Alternative layouts with 3 or 4 IPs are under study. The electron and positron bunches are collided under a large horizontal crossing angle of 30 mrad with a so-called crab-waist optics [10, 11]. The IR optics accommodates only one sextupole pair per final focus side, used for a local correction of the vertical chromaticity, with a cancellation of geometric aberrations. Reducing the strength of the outer sextupoles creates the crab waist [8]. This low number of strong sextupoles ensures a minimum amount of nonlinearity and a correspondingly large dynamic aperture. The FCC-ee synchrotron radiation power is limited to 50 MW per beam at all beam energies. The magnet strengths in the arcs are tapered so as to match the local beam energy. A common radiofrequency (RF) system is used for the  $\bar{f}$  running, where the maximum RF gradient is required, but the number of bunches is quite low, so that parasitic collisions in the RF straights can be avoided.

Key parameters of FCC-ee are compiled in Table 1. Figure 2 illustrates that the FCC-ee offers an attractive luminosity level over its entire centre-of-mass energy range from 90 to 365 GeV. From about 2 TeV onward a hypothetical muon collider (MAP-MC) is expected to yield the best performance. Between about 400 GeV and 1 or 2 TeV the linear colliders ILC and CLIC, respectively, appear optimally suited.

The FCC-ee design is based on proven techniques from past and present colliders, not pushing any key parameter (beam lifetime,  $\beta_y^*$ ,  $e^+$  production rate, SR photon energy)

## PRELIMINARY SIRIUS COMMISSIONING RESULTS

L. Liu<sup>†</sup>, M. B. Alves, F. C. Arroyo, J. F. Citadini, F. H. de Sá, R. H. A. Farias, J. G. R. S. Franco, R. J. Leão, S. R. Marques, R. T. Neuenschwander, A. C. S. Oliveira, X. R. Resende, A. R. D. Rodrigues, C. Rodrigues, F. Rodrigues, R. M. Seraphim, Brazilian Centre for Research in Energy and Materials (CNPEM)/Brazilian Synchrotron Light Laboratory (LNLS), Campinas, Brazil

### Abstract

Sirius is a 4<sup>th</sup> generation 3 GeV low emittance electron storage ring that is in final commissioning phase at the Brazilian Centre for Research in Energy and Materials (CNPEM) campus in Campinas, Brazil. Presently (April 2020) we have accumulated 15 mA of current, limited by vacuum, using a nonlinear kicker for injection. In this paper we report on the Sirius main commissioning results and main subsystems issues during installation and commissioning.

### INTRODUCTION

Sirius is a new light source in Brazil based on a low emittance 3 GeV electron storage ring with 518 m circumference. The storage ring natural emittance of 0.25 nm.rad is reached with twenty 5BA lattice cells and it can be further reduced to 0.15 nm.rad as insertion devices are added. Sirius will be an international multiuser research facility with up to 37 beamlines: 20 from permanent magnet superbends reaching peak magnetic field of 3.2 T (and therefore 19 keV critical photon energy); 4 from insertion devices at high beta sections and 13 at low beta sections. The low beta sections are optimized to maximize brightness from insertion devices by matching the electron beam and undulator radiation phase spaces. In these low beta sections, where the horizontal and vertical beta functions are simultaneously reduced to 1.5 m in the centre, small horizontal gap devices such as Delta undulators can be installed. Sirius main parameters are shown in Table 1 and the optical functions in Figure 1.

Table 1: Main Sirius Storage Ring Parameters

Parameter	Value	Unit
e-beam energy	3.0	GeV
Circumference	518.4	m
Lattice	20 x 5BA	
Hor. emittance (bare lattice)	0.25	nm.rad
Betatron tunes (H/V)	49.11 / 14.17	
Natural chrom. (H/V)	-119.0 / -81.2	
Energy spread	0.85e-3	
Energy loss/turn (dipoles)	473	keV
Damping times (H/V/L)	16.9/22.0/12.9	ms
Nominal current	350	mA

The injection into the storage ring will be based on conventional off-axis accumulation in the horizontal plane using a non-linear kicker (NLK). The injection system is composed of a 150 MeV Linac and a full-energy synchrotron booster with 497m circumference, built in the same tunnel and concentric with the storage ring. The booster has a very small emittance of 3.5 nm.rad at 3 GeV that is essential for a high injection efficiency using the NLK.

Commissioning activities were interrupted on last March 23<sup>rd</sup> due to the Covid-19 pandemic, when most of the staff switched to teleworking. We have reached 15 mA of accumulated current with off-axis injection in the horizontal plane using the NLK. This current is presently limited by vacuum. We are now slowly returning to work to continue with beam commissioning and proceed with installation of the first undulator for the protein crystallography beamline MANACÁ.

The Sirius project has effectively started in July 2012 when the decision to change to a low emittance 5BA lattice was taken, implying completely new components design. Installation of the accelerator subsystems in the machine tunnel started on May 2018 and the first turn in the storage ring with on-axis injection was achieved on Nov. 22<sup>nd</sup>, 2019. The first stored beam was obtained 3 weeks later, on Dec. 14<sup>th</sup>. Two days later, first light from a superbend was observed at the MOGNO beamline and first X-ray microtomography results were taken (see Figure 2). First beam accumulation with the NLK was obtained on Feb. 20<sup>th</sup>, 2020. Figure 3 shows a picture of the main accelerator tunnel.

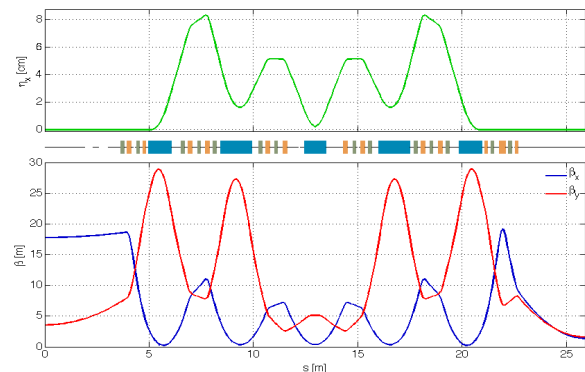


Figure 1: Sirius optical functions with a high-beta section on the left and a low-beta section on the right. The optics is 5-fold symmetric with 5 high-beta and 15 low-beta sectors. The centre dipole is a permanent magnet superbend.

<sup>†</sup> liu@lnls.br

# REVIEW OF REQUIRED PROOF-OF-PRINCIPLE EXPERIMENTS TOWARDS A MUON COLLIDER

Alessandro Variola, INFN – Sezione di Roma, P.le Aldo Moro 2, I-00185 Rome, Italy

## Abstract

The HEP scientific community is, at present, exploring different scenarios concerning the post LHC era. In fact, after the Higgs boson discovery, the future facility will require not only to improve the LHC and HL-LHC physics programs but also to continue the search for phenomena beyond the Standard Model into an extended energy domain. In this framework ideas and proposals, together with the results obtained in accelerator research, introduce a scenario where the feasibility of a multi-TeV muon collider should be explored.

This article will describe the advantages provided by the muon collider scheme. The proposed schemes will be shortly illustrated. The very important recent results obtained in proof-of-principle experiments will be subsequently described. Finally, for each scheme, the future possible directions for proof-of-principle experiments to demonstrate the muon collider feasibility will be presented.

## INTRODUCTION

The future challenges in the high energy colliders frontier, cannot be decoupled from the luminosity requirements keeping as fundamental constraint the necessity to build and operate the facility with a reasonable construction and operation budget. In this context a high energy muon collider should represent a true opportunity. In this framework a still-in-progress physics case has been elaborated [1] and this has been recently taken into account in the input for the European Strategy for Particle Physics Update 2020 in the Physics Briefing Book [2].

Different considerations make the muon collider option very attractive. First of all, the center of mass energy can be considerably reduced in respect to the p-p configuration where a significant fraction of the proton-beams energy in the interaction point is carried away by the partons contribution. Furthermore, the leptonic nature of the muons also assure a direct exploitation with a significant noise reduction, resulting in foster the muon potential not only as high energy but also as a precision collider. On the other side this solution presents definite advantages with respect to the  $e^+e^-$  configuration, mainly due to the about 200 mass scaling factor. This strongly relaxes the constraints in synchrotron radiation power emission and in the beamstrahlung effect that represent one of the main performance limitations respectively for the circular and linear lepton collider options. Finally, the luminosity parameter for the high energy configuration is linearly dependent from the energy at constant beam power, when compared to the constant behaviour of the linear collider option.

A final definitive assessment of the luminosity requirement should be delivered in a CDR phase where an extensive investigation of the physics channels should be carried

out. Nevertheless, basic considerations allow to fix a luminosity target of  $2 \cdot 10^{34} \text{cm}^{-2}\text{s}^{-1}$  at 3 TeV [3].

The undeniable advantages represented by the muon collider option are nevertheless challenged by the main limitation given by the muon  $2.2 \mu\text{s}$  at rest lifetime, rather short in a collider perspective. This is an important limiting factor namely at the muon production. In fact, muons bunches are produced with a very large 6D emittance and a limited number of particles per bunch limited by the primary beam power and the target technology. To provide a collider design matching the luminosity requirements, any applicable cooling technique needs, thereby, to show unprecedented efficiency to guarantee the emittance shrinking with a very fast process immediately after the production. This will permit the subsequent beam shaping, transport and post acceleration phases. Different techniques should also be envisaged to recombine muon bunches before a final cooling stage, to benefit of the luminosity quadratic dependence on the single bunch intensity. All these considerations underline the crucial aspect of the source design for the muon collider option. To provide a reliable design of a muon source integrating all the production, shaping, cooling and recombination phases represented for years the true challenge and it resulted in an important and long R&D effort sustained by the community. In this framework it is important to underline the muon collider R&D strong synergies with the neutrino physics programs.

## MUON COLLIDER SCHEMES

At present there are two main proposed scenarios for a muon collider facility the difference being essentially in the muon source design. The first has been elaborated in the framework of the US Muon Accelerator program (MAP) and it considers the muons as tertiary particles in the decays of the pions created by an intense proton beam interacting a heavy material target. The second, the LEMMA scheme, takes into account the process  $e^+e^- \rightarrow \mu^+\mu^-$  just above threshold for the muon generation considering a high energy positron beam impinging on a target. After the peculiar phases of bunch generation and emittance shaping associated to the specific production process, similar technical and design issues for the two schemes are found in the post acceleration stage. At the end, depending on the beam emittances, different collider ring design requirements are also considered.

## MAP: THE PROTON DRIVEN SCHEME

The Muon Accelerator Program [4] started in 2011 to develop the conceptual designs and to face all the technological R&D challenges associated to the Muon Colliders and Neutrino Factories. To establish the program priorities a baseline scheme was proposed [5]. The collider layout takes into account five different stages. The first includes

**MC3: Novel Particle Sources and Acceleration Techniques**

**A09 Muon Accelerators and Neutrino Factories**

# IFMIF/EVEDA RFQ BEAM COMMISSIONING AT NOMINAL 125 mA DEUTERON BEAM IN PULSED MODE

F. Grespan, L. Bellan, M. Comunian, E. Fagotti, A. Palmieri, A. Pisent, F. Scantamburlo  
INFN-LNL, Legnaro, Italy  
T. Akagi, Y. Hirata, K. Kondo, Y. Shimosaki, T. Shinya, M. Sugimoto, QST, Aomori, Japan  
P. Cara, IFMIF/EVEDA Project Team, Aomori, Japan  
H. Dzitko, A. Jokinen, A. Marqueta, I Moya, F4E, Garching, Germany  
B. Bolzon, N. Chauvin, J. Marroncle, CEA-IRFU, Gif-sur-Yvette, France  
A. Rodriguez Paramo, ESS Bilbao, Zamudio, Spain  
D. Jimenez-Rey, I. Podadera, CIEMAT, Madrid, Spain

## Abstract

In summer 2019 the IFMIF/EVEDA Radio Frequency Quadrupole (RFQ) accelerated its nominal 125 mA deuteron (D+) beam current up to 5 MeV, with 90% transmission for pulses of 1 ms at 1 Hz. The Linear IFMIF Prototype Accelerator (LIPAc) is a high intensity D+ linear accelerator; it is the demonstrator of the International Fusion Material Irradiation Facility (IFMIF). In particular the RFQ is the longest and most powerful ever operated. An intense campaign of measurements has been performed in Rokkasho to characterize several performances of this complex machine: transmission, emittances, energy spectrum and beam loading. The history and the results of the commissioning until this important project milestone are here described. An overview of the foreseen activities to be carried out to reach the CW operation is also presented.

## INTRODUCTION

The LIPAc RFQ is a CW linac, capable of delivering 125 mA of D+ beam at 5 MeV. The 10-m long, 175 MHz cavity is designed to accelerate a DC 100 keV, 130 mA D+ beam from the injector with transmission > 90% [1].

RFQ is installed in Rokkasho (Fig. 1) since April 2016. The low power RF characterization was concluded in September 2016. We installed the 8 power couplers in December 2016, checking the field by pick-up reading. After baking and connection to cooling system and to the 8 RF systems, RF conditioning started in July 2017 (Fig. 2). After a first period where some hardware and integration problems have been faced, in Spring 2018 the RF operation concentrated to stabilize the conditions for the proton beam injection [2].

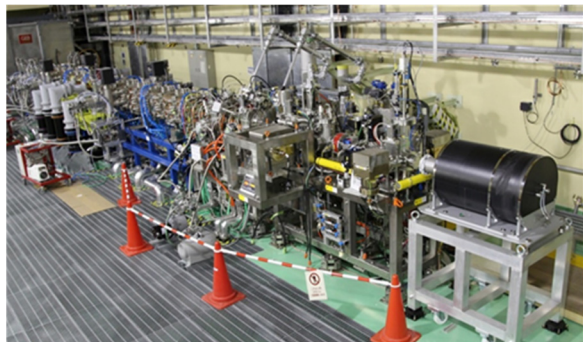


Figure 1: IFMIF/EVEDA LIPAc in Rokkasho.

In June 2018 first proton (H+) beam was successfully accelerated through the RFQ [3]. After maintenance, conditioning restarted in February 2019 (Fig. 2) with the goal of reaching the conditions to accelerate D+ [4]. First D+ injection was possible in March 2019, then we reached in July 132 kV-2.5 ms-20 Hz and in July 24th we achieved a 125 mA D+ current at 1 ms/1 Hz out the RFQ, with transmission > 90% (Fig. 3).

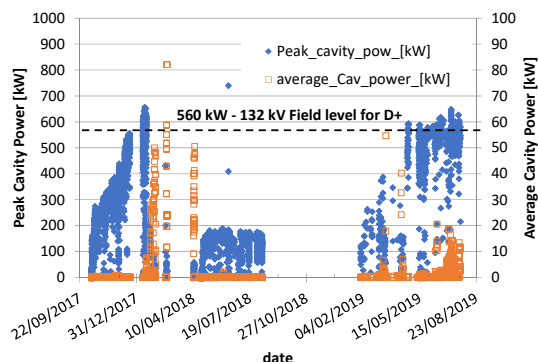


Figure 2: RF history of the RFQ (Sep. 2017 – Aug. 2019).

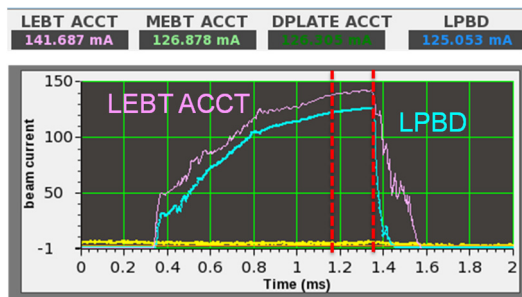


Figure 3: Image of the 125 mA D+ beam transmitted to the Low Power Beam Dump (LPBD).

## LIPAC CONFIGURATION

The configuration for beam commissioning of LIPAc RFQ is shown in Fig. 4. LEbt optics includes two solenoids (Sol#) with integrated steering magnet pairs (ST#). Diagnostics include Doppler-Shift Spectroscopy, a 4-grid analyser, an Allison-Scanner, a beam stop, two CCD beam profile monitors. Three cm from RFQ matching point, there is LEbt-ACCT. RFQ input plate includes an electron repeller (-3 kV). Cavity is maintained at 10<sup>-8</sup> mbar vacuum

# THE SIS100 RF SYSTEMS – UPDATES AND RECENT PROGRESS

J. S. Schmidt, R. Balß, M. Frey, P. Hülsmann, H. Klingbeil<sup>1</sup>, H. G. König,  
 U. Laier, D. E. M. Lens, A. Stuhl, GSI, Darmstadt, Germany  
<sup>1</sup>also at Technische Universität Darmstadt, Darmstadt, Germany

## Abstract

Within the FAIR (Facility for Antiproton and Ion Research) accelerator complex, the SIS100 synchrotron will provide high intensity proton to heavy ion beams to the various beam lines and storage rings. This paper presents the recent progress of the SIS100 overall RF system in its preparation towards installation. The RF system is split into four separate sub-systems with a significant number of RF stations. Each RF station consists of a ferrite or MA loaded cavity, a tetrode-based power amplifier, a switching mode power supply unit and various analogue or digital LLRF components for feedback and feedforward control. Fourteen ferrite cavities will generate the accelerating field, while nine cavities loaded with magnetic alloy ring cores are used for bunch compression. The barrier bucket system, which is used to apply a pre-compression of the beam, as well as the longitudinal feedback system for stabilization of beam oscillations will be realized by in total four cavities of the same type.

## INTRODUCTION

The Facility for Antiproton and Ion Research is an accelerator facility, which will provide high intensity beams for experimental programs with a wide range of particles including protons, all kinds of heavy ions as well as antiprotons. The existing accelerators of the GSI Helmholtzcentre for Heavy Ion Research will be used as injectors for the FAIR chain of accelerators, beam lines, storage rings and experimental stations. A major upgrade program is ongoing for the GSI machines as well.

The synchrotron SIS100 is the main accelerator of the FAIR complex. With a circumference of ~1.1 km the machine is designed to accelerate high intensity proton and heavy ion beams. Its name reflects the  $B\rho$  value of the ring, which will consist of a mixture of superconducting and normal conducting components [1]. The lattice is optimized for the broad ion spectrum between protons and uranium. Special care has been taken to control particle losses due to residual gas effects. The construction of the SIS100 complex is ongoing and advancing well [2].

Four different RF systems are being prepared for SIS100, namely: the acceleration system, the bunch compression system and the broadband systems: barrier bucket and longitudinal feedback with a total number of 27(+13) RF stations [3, 4]. The “(+13)” stations will be added only in a later stage of a SIS100 upgrade.

- 14 (+6) Acceleration System (AC)
- 9 (+7) Bunch Compression System (BC)
- 2 Barrier Bucket (BB)
- 2 Longitudinal Feedback (LF)

In a simplified view each RF station is a compound of one cavity, with its amplifier, power supply unit and LLRF system. Still, the system with all its details will be much more complex, including the gap periphery, water cooling, controls integration and much more. Figure 1 visualizes the distribution of the RF stations along the SIS100 ring. The RF stations are located in all sectors (except sector 5, where the extraction system is located). For all of those systems the goal is to provide robust components for reliable operation of the RF stations.

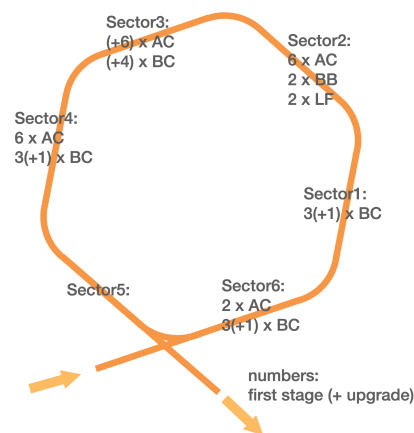


Figure 1: The distribution of the RF stations along the SIS100 ring. The numbers in brackets represent a later stage of a SIS100 upgrade

## THE ACCELERATION SYSTEM

The 14(+6) RF stations of the AC system will accelerate ions in fast ramping cycles. The cavities are designed to provide high acceleration gradients of 20 kVp per cavity in cw operation. The design is based on the SIS18 design with two ferrite core stacks operating against one ceramic gap to provide the acceleration voltage. One of the challenges is to control degrading effects like dynamic and quality loss effects (ferrite characteristics) [5]. The tuning rates of  $\geq 10$  MHz/s lead to the need of a dedicated frequency tuning system.

The main parameters of the AC RF stations are:

- Continuous wave operation (cw)
- Frequency range from 1.1 MHz to 3.2 MHz
- Nominal voltage of 20 kVp
- Impedance seen by the beam  $< 2$  kOhm
- Cavity length of 3 m
- Tuning rate  $\geq 10$  MHz/s

The acceleration system is being realized by RI Research Instruments GmbH in collaboration with Ampegon Power Electronics AG for the power supply units. The first-of-series RF station has been successfully tested in a test stand

Content from this work may be used under the terms of the CC BY 3.0 licence (© 2019). Any distribution of this work must maintain attribution to the author(s), title of the work, publisher, and DOI

# LONG-TERM BEAM POSITION AND ANGLE STABILITIES FOR THE J-PARC MAIN RING SLOW EXTRACTION

M. Tomizawa\*, Y. Arakaki, T. Kimura, S. Murasugi,  
R. Muto, K. Okamura, E. Yanaoka, ACCL, KEK, Tsukuba, Japan  
Y. Komatsu, Y. Shirakabe, IPNS, KEK, Tsukuba, Japan

## Abstract

A 30 GeV proton beam accelerated in the J-PARC Main Ring (MR) is slowly extracted by the third integer resonant extraction and delivered to the hadron experimental hall. A unique dynamic bump scheme for the slow extraction has been applied to reduce the beam loss. The current extraction efficiency is very high, 99.5%. However, the dynamic bump scheme is sensitive to the beam orbit angle at the first electrostatic septum (ESS1). The orbit angle of the dynamic bump must be sometimes readjusted to keep such a high efficiency. A long term stability of the orbit depending to momentum has been investigated.

## INTRODUCTION

A high-intensity proton beam accelerated in the J-PARC main ring (MR) is slowly extracted by the third integer resonant extraction and delivered to the hadron experimental hall to drive various nuclear and particle physics experiments [1]. Most of the proposed experiments are best performed using a coasting beam without an RF structure and a uniform beam intensity during the extraction time. One of the critical issues in slow extraction (SX) of a high intensity proton beam is an inevitable beam loss caused by the extraction process at septum devices. A unique dynamic bump scheme for the slow extraction has been applied to reduce the beam loss [2]. The layout of J-PARC MR Slow extraction devices is shown in Fig. 1.

The beam power of 30 GeV slow extraction has achieved to 51 kW at 5.2s cycle in current physics runs. The extraction efficiency is very high, typically 99.5%. However, the dynamic bump scheme is sensitive to the beam orbit angle at the first electrostatic septum (ESS1). The orbit angle of the dynamic bump must be sometimes readjusted to keep such a high efficiency. A long-term stabilities of the orbit and the relative momentum have been investigated in this paper. The work in this paper is useful for a diffuser [3] and/or a silicon bend crystal [4] to achieve further high slow extraction efficiency introduced in future. They could be more sensitive to the orbit and momentum shifts.

## CURRENT SLOW EXTRACTION PERFORMANCES

The momentum pattern of the current slow extraction is shown in Fig. 2. The repetition cycle is 5.2 s, in which the flat top length is 2.61 s. The proton number per cycle is  $5.6 \times 10^{13}$  ppp corresponding to 51 kW. The extraction

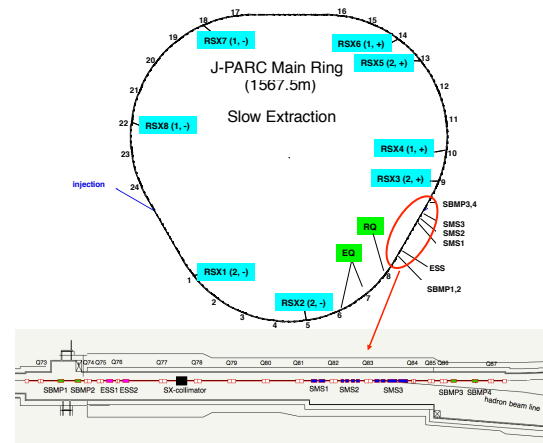


Figure 1: Layout of J-PARC slow extraction devices.

efficiency is very high, 99.5% [5,6]. The typical spill length and spill duty factor is 2 s and 50%, respectively [6]. In the current beam power, the transverse instability during the debunch process to obtain an uniform time structure is serious. To solve this problem, the beam is injected to the RF buckets with phase offset of 50–60 degree [5]. The resultant momentum width is spread to  $\sim 0.5\%$  in full width at the flat top.

The dynamic bump orbit tuning associated with the position and angle of the electrostatic septa (ESS1 and ESS2) and the magnetic septa (SMS1 and SMS2) is the most important to obtain a high extraction efficiency. Figure 4 shows extraction efficiency as a function of the bump orbit angle at the entrance of the ESS1. The bump orbit angle is for the end of extraction and the actual bump orbit angle is shifted so as to superimpose the extraction arms from the separatrices

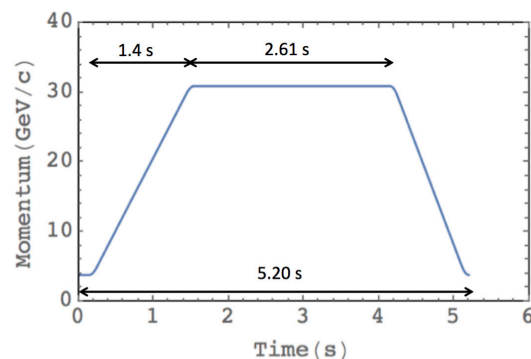


Figure 2: Momentum pattern of MR slow extraction operation.

\* masahito.tomizawa@kek.jp

# MICROBUNCH ROTATION AS AN OUTCOUPLING MECHANISM FOR CAVITY-BASED X-RAY FREE ELECTRON LASERS\*

R. A. Margraf<sup>†1</sup>, Z. Huang<sup>1</sup>, J. P. MacArthur, G. Marcus  
SLAC National Laboratory, Menlo Park, USA  
<sup>1</sup>also at Stanford University, Stanford, USA

## Abstract

Electron bunches in an undulator develop periodic density fluctuations, or microbunches, which enable the exponential gain of power in an X-ray free-electron laser (XFEL). For certain applications, one would like to preserve this microbunching structure of the electron bunch as it experiences a dipole kick which bends its trajectory. This process, called microbunch rotation, rotates the microbunches and aligns them perpendicular to the new direction of electron travel. Microbunch rotation was demonstrated experimentally by MacArthur et al. with soft x-rays [1] and additional unpublished data demonstrated microbunch rotation with hard x-rays. Further investigations into the magnetic lattice used to rotate these microbunches showed that microbunches can be rotated using an achromatic lattice with a small R56, connecting this technique to earlier studies of achromatic bends. Here, we propose and study a practical way to rotate Angstrom-level microbunching as an out-coupling mechanism for the Optical Cavity-Based X-ray FEL (CBXFEL) project at SLAC.

## CAVITY-BASED XFELS AND THE CBXFEL PROJECT

Current state-of-the-art XFELs, including the LCLS at SLAC, are SASE (Self-Amplified Spontaneous Emission) XFELs, as depicted in Fig. 1A. A several GeV electron beam passes through an undulator, a series of alternating north-south magnets which rapidly bend the e-beam trajectory back and forth. An e-beam/radiation collective instability occurs when this oscillating electron beam interacts with light at a resonant wavelength, developing periodic density modulations, “microbunches,” which increase the coherence of resonant X-ray synchrotron radiation emitted by the electrons. In a SASE XFEL, the light which seeds the XFEL arises from noise. This light is incoherent and low intensity, thus many undulators are required to microbunch the electron beam and produce bright X-rays. The resultant X-ray pulse is transversely coherent, but longitudinally chaotic, with a longitudinal coherence length inversely proportional to the spectral bandwidth of the XFEL amplifier,  $l_{coh} \sim \frac{1}{\sigma_\omega}$  [2]. This longitudinal coherence can be increased by seeding with X-rays of a narrower bandwidth than the XFEL amplifier. Lacking compact coherent X-ray sources, one solution

is to use monochromatized X-rays generated from SASE to seed the XFEL process, as is done in a cavity-based XFEL.

The CBXFEL Project will demonstrate two-pass gain in the LCLS-II hard X-ray undulator line using the LCLS copper linac in two-bunch mode. Four diamond (400) mirrors will wrap seven undulators (~ 35 m) to form a rectangular optical cavity as depicted in Fig. 1B. Hard X-rays at 9.83 keV from the first bunch will Bragg reflect and return to seed a trailing fresh electron bunch on the subsequent pass.

CBXFEL will develop technologies to enable future production-level cavity-based XFELs which leverage the high repetition rate (1 MHz) and electron energy (8 GeV) of the LCLS-II High Energy (HE) upgrade [3]. These cavities may wrap the entire 130 m undulator line at SLAC such that the photon cavity round trip time matches the arrival of MHz electron bunches.

Table 1 summarizes the projected outputs of such production-level facilities in two modes, X-ray Regenerative Amplifier FEL (XRAFEL) and X-ray FEL Oscillator (XFEL). XRAFEL is a high gain system, regenerating a large percentage of the X-ray power on each pass through the cavity. XRAFEL can produce >5 times the peak power and 100 times the energy resolution of a SASE FEL, while maintaining short pulse lengths. XFEL is a low-gain system which builds up X-ray power over many passes. XFEL produces X-ray pulses with 10,000 times narrower energy resolution, and 1000 times higher average spectral brightness, with the trade-off of longer X-ray pulses. Both have high longitudinal coherence and stability, replacing chaotic arrival times of SASE spikes.

Table 1: Projected Cavity-based XFEL Properties [4, 5]

	SASE	XRAFEL	XFEL
<b>Gain</b>	High	High	Low
<b>Passes to Saturation</b>	1	10's	100's
<b>Peak Power</b>	10 GW	>50 GW	10 MW
<b>Average Power</b>	100 W (1 MHz)	10 W (10 kHz)	20 W (1 MHz)
<b>Bandwidth</b>	10 eV	0.1 eV	20 meV
<b>Average Spectral Brightness</b> ( $\frac{\text{photons}}{\text{s mm}^2 \text{ mrad}^2 \cdot 1\% \text{ BW}}$ )	10 <sup>25</sup>	10 <sup>26</sup>	10 <sup>28</sup>
<b>Pulse Length</b>	1-100 fs	20 fs	1 ps
<b>Temporal Stability and Coherence</b>	Poor	Excellent	Excellent

\* This work was supported by the Department of Energy, Laboratory Directed Research and Development program at SLAC National Accelerator Laboratory, under contract DE-AC02-76SF00515.

<sup>†</sup> rmargraf@stanford.edu



# ON-AXIS BEAM ACCUMULATION BASED ON A TRIPLE-FREQUENCY RF SYSTEM

Gang Xu, Shichang Jiang\*

Key Laboratory of Particle Acceleration Physics and Technology,  
Institute of High Energy Physics, Chinese Academy of Sciences,  
University of Chinese Academy of Sciences, 100049 Beijing, China

## Abstract

Considering the incompatible off-axis injection scheme on the newly constructed light sources, we have proposed a new on-axis accumulation scheme based on the so-called triple-frequency RF system. By means of additional second harmonic cavities, the original static longitudinal acceptance will be lengthened, which will provide the sufficient time to raise a full-strength kicker pulse. Through imposing the specific restriction on the RF parameters, the final bunch length can also be stretched to satisfy the functions of the conventional bunch lengthening system. In this paper, we will move on to explain how to build this complex triple-frequency RF system, and present the relevant simulation works.

## INTRODUCTION

One of the intrinsic characteristics of advanced light sources, is their small dynamic aperture, which brings new challenges for the design of corresponding injection scheme [1]. Due to this specific characteristic, conventional off-axis injection schemes might be incompatible. Several new injection schemes are being designed, in which swap-out injection is a mature case and it will be utilized in the latest light sources [2, 3]. Enlightened by few on-axis injection schemes, we also proposed a new on-axis accumulation scheme, which is based on a triple-frequency RF system, consisting of fundamental, second harmonic and third harmonic cavities [4]. Compared to the conventional bunch lengthening system, normally indicating a double-frequency RF system, the extra harmonic cavities will help lengthen the original static longitudinal acceptance. The local extreme point in the potential curve, corresponding to the fixed point in the longitudinal acceptance, is away from the synchrotron phase. As well as the time interval between the circular bunch and the outermost injection point, we expect this value, employing general lattice parameters of the fourth-generation light sources, could be larger if the “golf club” effect is taken into consideration [5]. Based on the current design, the time interval between this two points, can be lengthened to nearly 2 ns, and this value in the single frequency RF system or the double-frequency RF system is less than 1.5 ns. Furthermore if considering the energy loss per turn is related to the energy spread, this time interval is able to be increased about 10% to 15%. So long as the design of the kicker is compatible with the above time

limit, there will not be any disturbance to the circular bunch in the whole injection process. Also the injection can be done in multiturn, when the last injected bunch merged to the synchrotron phase, the next kicker pulse can be raised again. This injection scheme also relieve the design for the booster, if a high charge bunch is needed in the storage ring, and all the RF parameters can remain unchanged during the injection. In this paper, we will explain how to build such triple-frequency RF system, and present the relevant simulation results, in allusion to a typical fourth-generation light source.

## THE CONSTRUCTION OF THE TRIPLE-FREQUENCY RF SYSTEM

Without radiation damping, the single-particle motion while considering the triple-frequency RF system,

$$\begin{aligned}
 H(\phi, \delta; t) = & \frac{h_f \omega_0 \eta}{2} \delta^2 + \frac{\omega_0 e}{2\pi E_0 \beta^2} \left[ \sum_{i=1}^{N_f} V_f^i \cos(\phi + \phi_f^i) \right. \\
 & + \frac{h_f}{h_1} \sum_{j=1}^{N_{h_1}} V_{h_1}^j \cos\left(\frac{h_1}{h_f} \phi + \phi_{h_1}^j\right) \\
 & \left. + \frac{h_f}{h_2} \sum_{k=1}^{N_{h_2}} V_{h_2}^k \cos\left(\frac{h_2}{h_f} \phi + \phi_{h_2}^k\right) + \phi U_0 \right], \quad (1)
 \end{aligned}$$

where  $\phi$  and  $\delta$  are a pair of canonical variables with respect to the time variable  $t$ ,  $\omega_0 = 2\pi c/C$  is the angular revolution frequency of the synchrotron particle,  $c$  is the speed of light,  $C$  is the circumference of the storage ring.  $\eta = \alpha_c - 1/\gamma^2$ ,  $\beta = \sqrt{1 - \gamma^2}$ , where  $\alpha_c$  is the momentum compaction factor of the storage ring,  $\gamma$  is the relativistic factor. Suppose there are  $N_f$  fundamental cavities with a harmonic number  $h_f$ ,  $N_{h_1}$  harmonic cavities with a harmonic number  $h_1$ , and  $N_{h_2}$  harmonic cavities with a harmonic number  $h_2$ .  $V_f^i$ ,  $V_{h_1}^j$  and  $V_{h_2}^k$  are the voltages of the  $i$ -th fundamental cavity, the  $j$ -th 2nd harmonic cavity and the  $k$ -th 3rd harmonic cavity respectively.  $\phi_f^i$ ,  $\phi_{h_1}^j$  and  $\phi_{h_2}^k$  are the phases of the synchrotron particle relative to the above cavities.

According to the natural mathematical features of the potential curve, and lengthening the bunch longitudinally, we have several restrictions,

$$P(\phi_b) = P_{max}, P'(\phi_b) = 0, P''(\phi_s) = 0. \quad (2)$$

In which function  $P(\phi)$  is the beam potential,  $\phi_b$  is the fixed point in the longitudinal acceptance, corresponding to the

\* jiangsc@ihep.ac.cn

# LONGITUDINAL STABILITY WITH LANDAU CAVITIES AT MAX IV

F. J. Cullinan\*, Å. Andersson, P. F. Tavares, MAX IV Laboratory, Lund, Sweden

## Abstract

The use of Landau cavities was foreseen for both the 1.5 GeV and 3 GeV storage rings at the MAX IV facility from conception. Along with increasing the Touschek lifetime and reducing the emittance degradation due to intrabeam scattering, their purpose is to stabilise the beam in the longitudinal plane. They now play a crucial role in the everyday operation of the two storage rings. This paper outlines the current status and the aspects of longitudinal beam stability that are affected, positively or negatively, by the presence of Landau cavities. Their effectiveness in the two storage rings is also compared.

## INTRODUCTION

MAX IV is a synchrotron light source facility in Lund, Sweden. It includes two storage rings: one at 1.5 GeV and another at 3 GeV whose circumference is more than five times larger than the first. A linac injects both rings at full energy and also functions as a light source for the generation of short x-ray pulses. The smaller of the two storage rings has a double-bend achromat lattice while the larger ring, with its multibend-achromat lattice, is a fourth-generation storage ring that is capable of delivering ultrahigh-brightness X-rays because of the low bare-lattice horizontal emittance of 330 pm rad. Both rings operate in top-up during delivery of light to users. Table 1

Table 1: Selected machine parameters of the MAX IV storage rings. The lengths of the lengthened bunches are for 500 mA with flat potential conditions.

Parameter	1.5 GeV Ring	3 GeV Ring
RF frequency MHz		100
Landau-cavity harmonic		3
Design current mA		500
Landau-cavity... ...shunt impedance MΩ		2.5
...quality factor		20800
Main-cavity loaded... ...shunt impedance MΩ	0.569	0.310
...quality factor	6760	3690
Natural bunch length ps	49	40
Lengthened bunch ps	195	196
Harmonic number	32	176
Momentum compaction	0.000306	0.003055
Bare-lattice energy loss per turn keV	363.8	114.4
Number of... ...main cavities	2	5
...Landau cavities	2	3

\* francis.cullinan@maxiv.lu.se

lists the main parameters of the two storage rings with focus on the RF cavities which are at the same frequency in both rings [1].

Each ring has a double RF system with Landau cavities at the third harmonic of the main RF. The Landau cavities are made of copper, like the main RF cavities, and are passively loaded by the beam itself. In bunch-lengthening mode, the Landau cavities are detuned so that the resonant frequency of their fundamental mode higher than the RF harmonic and to increase or decrease the field level, the detuning is decreased or increased respectively. During operation, autotuning in the low-level RF is used to maintain the cavity voltage at a fixed value [2]. The variation along the bunch of the voltage in the Landau cavities is opposite to that in the main RF cavities so that the total RF voltage is flatter than with a single-RF system. This leads to longer electron bunches which reduces the scattering of electrons within the bunch and this means lower emittance and energy spread and a longer beam lifetime. Furthermore, lengthening the bunches with Landau cavities increases the threshold of certain collective instabilities in both the transverse [3] and longitudinal planes. This paper deals mostly with longitudinal coupled-bunch instabilities in the longitudinal plane, which are the dominant instabilities in both storage rings at MAX IV. These are driven by higher-order modes (HOMs) in the main and Landau cavities, which have no HOM dampers. Landau-cavity bunch lengthening is advantageous in this regard because of two reasons. The first is that the longer bunches have lower form-factors at the frequencies of the higher-order modes and so excite them less strongly. The second is the large spread in the synchrotron tune within the bunches, which means Landau damping of collective instabilities.

The two storage rings at MAX IV present a rare opportunity because the impedances driving the dominant instability in each ring are so similar, differing only in magnitude due to the different cavity numbers. Furthermore, the two rings have been commissioned and ramped in current more or less simultaneously and the observation of longitudinal instabilities during this time differed considerably. A comparison of the current statuses of the two rings in terms of longitudinal stability is listed in Table 2.

## LONGITUDINAL STABILITY

This section summarises the different issues in the two storage rings that affect the longitudinal stability and how they are dealt with.

### Robinson Mode Coupling

For bunch lengthening, Landau cavities must be tuned slightly higher than the third harmonic of the main RF. At this frequency, they destabilise the Robinson dipole and

# HOLLOW ELECTRON BEAMS IN A PHOTOINJECTOR

A. Halavanau<sup>1</sup>, C. Mayes<sup>1</sup>, Y. Ding<sup>1</sup>, S. Baturin<sup>2</sup>, P. Piot<sup>2,3</sup>

<sup>1</sup>SLAC National Accelerator Laboratory, Menlo Park, CA 94025, USA

<sup>2</sup>Northern Illinois University, DeKalb, IL 60115, USA

<sup>3</sup>Argonne National Laboratory, Lemont, IL 60439, USA

## Abstract

Photoinjectors have demonstrated the capability of electron beam transverse tailoring, enabled by microlens array (MLA) setups. For instance, electron beams, transversely segmented into periodic beamlet formations, were successfully produced in several experiments at Argonne Wakefield Accelerator (AWA). In this proceeding, we discuss the necessary steps to demonstrate the hollow electron beam generation, with an arbitrary diameter and width with MLAs. We also present beam dynamics simulations and highlight key features of the hollow beam transport in LCLS copper linac.

## INTRODUCTION

Hollow electron beams have been well known since 1960s, but due to multiple instabilities pointed out by early researchers [1–12] they have been largely forgotten. Nowadays, the most promising application of the hollow electron beams is proton beam collimation. This novel technique is soon to be implemented at Fermilab Accelerator Science and Technology (FAST) facility and later on at the Large Hadron Collider (LHC) [13–17]. The required hollow electron beams are generated in a special low energy source, mostly incompatible with a conventional accelerator. In this proceeding, we are exploring a different approach. We consider a nominal photoinjector configuration, e.g., the LCLS copper linac photoinjector, and modify the UV laser transverse profile employing spatial shaping techniques [18, 19]. Typically, transverse shaping is performed at some point upstream of the photocathode, which is then imaged onto the photocathode surface with a transport lens system. With the MLA shaping, for instance, one can apply a circular intensity mask at the homogenization point of the MLA, thus controlling parameters of the hollow beam. Other possibilities include the use of digital micromirror devices, axicon lenses, and more exotic Laguerre-Gaussian ( $LG_{0l}$ ) modes of the laser.

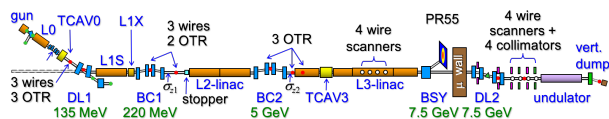


Figure 1: LCLS copper linac hard X-ray beamline.

## LCLS PHOTOINJECTOR AND COPPER LINAC SIMULATION

In this section we provide the results of numerical beam dynamics simulations of the entire LCLS copper linac hard X-ray (HXR) beamline, starting at the photocathode, and up to the HXR undulator entrance. LCLS copper linac photoinjector is a 135 MeV machine that comprises of 1.6 cell S-band RF gun with copper cathode and is operating at 120 Hz repetition rate. It is followed by multiple normal conducting travelling wave S-band accelerating structures. For a detailed description of the machine see Ref. [20]. Currently the primary purpose of the LCLS copper linac photoinjector is to produce electron beams for LCLS XFEL operations. The 135 MeV electron beam is then further accelerated in 1 km long linac with the total maximum energy of 14 GeV. We performed our hollow beam numerical study in the LCLS copper linac at a 7.5 GeV beam energy. We note that in the photoinjector the beam is matched into the copper linac via a quadrupole lattice, yielding several betatron oscillations in both vertical and horizontal planes. According to previous studies, such oscillations, in combination with space-charge forces, often lead to a hollow beam break up. An overall layout of the beamline is reported in Fig. 1 and a typical beam envelope evolution in the LCLS photoinjector is presented in Fig. 2. We point out that the nature of instability, destroying the hollow shape, is similar to the one observed in recent coherent electron cooling studies (CeC) at Brookhaven National Laboratory [21]. For our studies we utilized conventional IMPACT-T beam physics code [22]. A detailed description of IMPACT-T 3D space-charge algorithm and its comparison to other codes is available in Refs. [23–25]. As a guidance for initial simulation, the bunch charge was defined as

$$Q = 9 \text{ pC} \cdot \eta \frac{E_z}{\text{MV/m}} \frac{A}{\text{mm}^2} \quad (1)$$

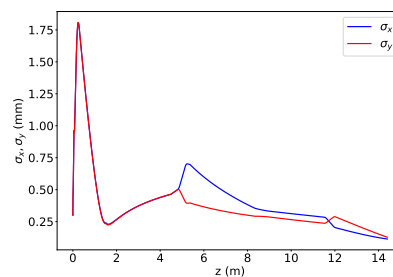


Figure 2: A typical electron beam size evolution in LCLS copper linac photoinjector.

# ADAPTIVE FEEDBACK AND MACHINE LEARNING FOR PARTICLE ACCELERATORS \*

Alexander Scheinker<sup>†</sup>, Los Alamos National Laboratory, Los Alamos, NM, USA

## Abstract

The precise control of charged particle beams, such as an electron beam's longitudinal phase space as well as the maximization of the output power of a free electron laser (FEL), or the minimization of beam loss in accelerators, are challenging tasks. For example, even when all FEL parameter set points are held constant both the beam phase space and the output power have high variance because of the uncertainty and time-variation of thousands of coupled parameters and of the electron distribution coming off of the photo cathode. Similarly, all large accelerators face challenges due to time variation, leading to beam losses and changing behavior even when all accelerator parameters are held fixed. We present recent efforts towards developing machine learning methods along with automatic, model-independent feedback for automatic tuning of charge particle beams in particle accelerators. We present experimental results from the LANSCE linear accelerator at LANL, the EuXFEL, AWAKE at CERN, FACET-II and the LCLS.

## INTRODUCTION

Particle accelerators are complex systems with many coupled components including hundreds of radio frequency (RF) accelerating cavities and their RF amplifiers as well as thousands of magnets for steering and focusing charged particle beams and their power sources. Accelerator designs are initially optimized by utilizing analytical beam physics knowledge and simulation studies. Once accelerators are built their performance does not exactly match the theory and models on which their design is based.

The differences between actual and designed systems are due to factors including idealized analytical studies that make simplifying assumptions and misalignment of accelerator components. Beyond not matching their designs, accelerator components and their beams drift unpredictably with time: 1). RF and magnet system amplifiers, power sources, and reference signals drift with temperature and suffer random perturbations from the noise within the electrical grid; 2). The initial 6D  $(x, y, z, p_x, p_y, p_z)$  phase space distribution of the beams entering accelerators from ion sources or photo cathodes drift and change unpredictably with time.

Most existing diagnostics are either destructive in nature or only provide beam-averaged measurements. Transverse deflecting cavities (TCAV), which can measure the longitudinal phase space (LPS) of relativistic electron bunches, destroy those bunches in the measurement process [1]. Beam position monitors (BPM) are non-invasive but only provide

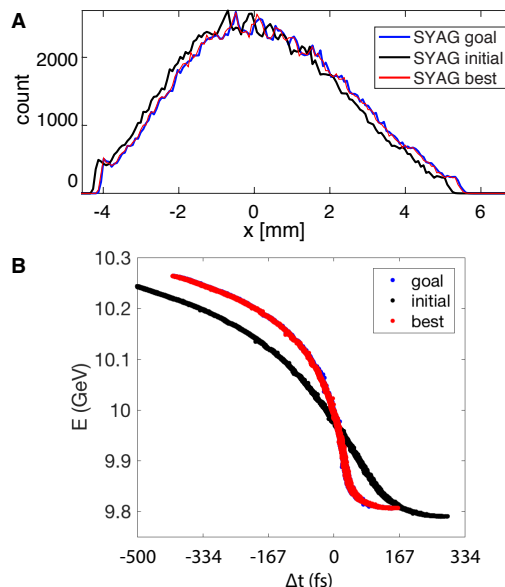


Figure 1: The adaptive model is tuned to match SYAG-based measurements of energy spread spectra (A). Once the modeled (red) and measured (blue) spectra converge the LPS of the measured beam is predicted almost exactly (B).

bunch-averaged position measurements and beam loss monitors provide no beam data beyond specifying a rough estimate of beam loss within a large region of an accelerator.

Because accelerators are uncertain and time-varying systems tuning and optimization require many hours of manual tuning. Tuning is especially challenging at older facilities with limited diagnostics such as the LANSCE linear accelerator at LANL [2], at facilities that must generate extremely short and intense beams such as FACET-II [3], and at facilities which require complex and precisely aligned interactions between multiple beams such as AWAKE [4]. Even the latest and most advanced facilities, especially when making large configuration changes to accommodate various experiment setups such as what must routinely take place at advanced FEL facilities such as the LCLS [5], LCLS-II [6], EuXFEL [7], PALFEL [8], and the SwissFEL [9].

Adaptive feedback and machine learning (ML) approaches are growing in popularity for particle accelerator for magnet tuning [10], non-invasive TCAV LPS diagnostics based on adaptive models at FACET [11], LPS diagnostics based on neural networks (NN) at SLAC [12], FEL light output power maximization at the LCLS and at the EuXFEL [13], surrogate modeling [14], detecting faulty BPMs and for optics corrections at the LHC at CERN by utilizing isolation forest techniques and NNs [15, 16], beam tuning at the SPEAR3 light source via Gaussian processes [17], and

\* This research was supported by a LANL Laboratory-Directed Research and Development (LDRD) Director's Initiative project 20200410DI.

<sup>†</sup> ascheink@lanl.gov

# SAFETY SYSTEM FOR THE RESPECT OF NUCLEAR REQUIREMENTS OF SPIRAL2 FACILITY

P. Anger<sup>†</sup>, V. Cingal, J.C. Pacary, S. Perret-Gatel, A. Savalle  
GANIL Laboratory, Caen, France

## Abstract

The SPIRAL2 Facility at GANIL is based on the construction of a superconducting, CW, ion LINAC (up to 5 mA - 40 MeV deuteron beams and up to 1 mA - 14.5 MeV/u heavy ion beams) with two experimental areas called S3 and NFS.

For safety system, SPIRAL2 project system engineering sets up a specific reinforced process, based on V-Model, to validate, at each step, all the requirements (technical, nuclear safety, quality, reliability, interfaces...) from the functional specifications to the final validation.

Since 2016, safety devices have been under construction and in test phase. These tests which are pre-requisites to deliver the first beam demonstrated that both functional and safety requirements are fulfilled. Currently, all of them are in operation for the LINAC and NFS commissioning phases.

This contribution will describe the requirements, the methodology, the quality processes, the technical studies for two system examples, the failure mode and effects analysis, the tests, the status and will propose you a feedback.

## INTRODUCTION

GANIL is a nuclear physic laboratory based in France since 1980 and SPIRAL2 is a new facility to extend the capability of GANIL.

Officially approved in May 2005, the SPIRAL2 radioactive ion beam facility (Fig. 1) is based on two phases: A first one including the accelerator, the Neutron-based research area (NFS) and the Super Separator Spectrometer (S3) dedicated to heavy nuclei studies, and a second one including the RIB production process and building, and the low energy RIB experimental hall called DESIR [1, 2].

In 2013, due to budget restrictions, the RIB production part was postponed, and DESIR was planned as a continuation of the first phase.

The first phase SPIRAL2 facility is now built and Desir is under study. The accelerator is installed [3]. The French safety authority agreement is now validated since 2019 according the validation of all safety system and the accelerator is under testing. A first p-beam was accelerated in the LINAC at 33 MeV and injected to experimental hall (NFS) at the end of 2019 [4]. Actually, the accelerator is under commissioning with nominal current at high duty cycle.

<sup>†</sup> pascal.anger@ganil.fr

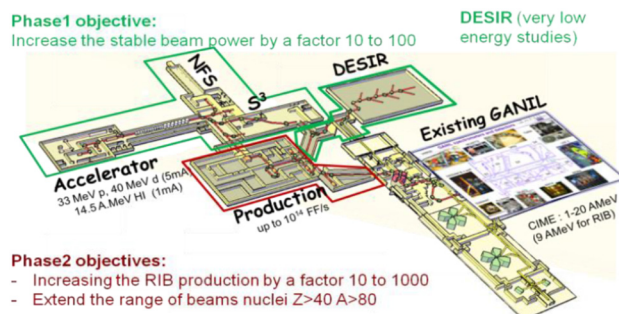


Figure 1: SPIRAL2 project layout, with experimental areas and connexion to the historical GANIL facility.

## PROBLEMATIC

The GANIL/SPIRAL2 facility is considered as an “INSTALLATION NUCLEAIRE DE BASE” (INB), administrative denomination for nuclear facilities according to the French law. The GANIL is under the control of the French Nuclear Safety Authority. The classification of the SPIRAL2/GANIL facility in the INB field is due to the characteristics of the beams at the last acceleration state and the use of actinide target.

The goals are to protect workers, public and environment against all identified risks (in normal running, the maximum individual dose is fixed to 1 mSv per year for a worker, and for the most exposed public in the external environment, the impact of the installation is fixed to a maximum value of 10  $\mu$ Sv per year).

Concrete building (14.000 m<sup>3</sup>) and an 8 meters underground beam axis, without beam power control is not sufficient for protection against external exposure to ionizing radiation. Active safety systems are then required to control beam losses as well as the operating range.

## METHODOLOGY

The objective was to provide all safety system according to the safety requirements (functionalities, independence, dependability, and quality insurance) and according to the beam operation constraints (in particular the safety systems availability).

Since 2010, we have established a system engineering management. It is a very structuring approach for a complex project. The Systems engineering focuses on the needs definition for the customer and for the functional requirements, from the beginning of the cycle (V Model Fig. 2), by documenting the requirements, then with the synthesis of the conception (design), the realization and the validation of the system.

# MACHINE LEARNING TECHNIQUES FOR OPTICS MEASUREMENTS AND CORRECTIONS

E. Fol<sup>\*</sup>, G. Franchetti<sup>†\*</sup>, R. Tomás, CERN, 1211 Geneva 23, Switzerland  
also at <sup>\*</sup>Johann-Wolfgang Goethe University, 60438 Frankfurt am Main, Germany  
<sup>†</sup> GSI Helmholtzzentrum für Schwerionenforschung, 64291, Darmstadt, Germany

## Abstract

Recently, various efforts have presented Machine Learning (ML) as a powerful tool for solving accelerator problems. In the LHC a decision tree-based algorithm has been applied to detect erroneous beam position monitors demonstrating successful results in operation. Supervised regression models trained on simulations of LHC optics with quadrupole errors promise to significantly speed-up optics corrections by finding local errors in the interaction regions. The implementation details, results and future plans for these studies will be discussed following a brief introduction to ML concepts and its suitability to different problems in the domain of accelerator physics.

## INTRODUCTION

Accelerator physics problems build a wide range of complex numerical and analytical tasks, e.g. modeling of different aspects of beam behavior, machine performance optimization, measurements data acquisition, and analysis. The growing complexity of modern and future accelerators provides the motivation to explore alternative techniques, which can complement traditional methods or even surpass their performance and offer opportunities to build more efficient and powerful tools. Machine Learning (ML) techniques have been introduced into numerous scientific and industrial areas demonstrating human-surpassing performance in pattern recognition, forecasting, and optimization tasks. These ML concepts can find analogies in the domain of accelerator physics as it will be shown in the following.

Considering the particular case of optics measurements and corrections, traditional techniques meet their limitation, e.g. dealing with erroneous signal artefacts that cannot be related to known patterns in the measurements data. Unsupervised ML techniques cover these limitations by learning the thresholds for anomalies detection directly from the given data as it will be shown on the example of identification of beam position monitors (BPM) faults. Another example is the optics perturbations caused by magnetic gradient field errors, which have to be corrected in order to control the beam optics. Supervised ML models built on simulations of the optics perturbed with thousands of realisations of quadrupolar magnet errors can predict the actual magnetic errors present in the machine, providing additional information for the computation of correction settings. Due to hardware and electronics issues, the signal measured at the BPMs suffers from noise that produces uncertainties in the

optics functions reconstructed from the harmonic analysis of BPM turn-by-turn readings. For this problem a special kind of Neural Networks named Autoencoder has been applied as a denoising technique improving the precision of phase measurements, thus potentially leading to more precise computed corrections based on the measured optics. The following section presents a short overview on latest achievements of applying ML to different types of particle accelerators.

## MACHINE LEARNING CONCEPTS IN ACCELERATOR PHYSICS

The concept of ML is known since the middle of the last century. The definition of ML is referred to computer programs and algorithms that automatically improve with experience by learning from examples with respect to some class of task and performance measures without being explicitly programmed [1]. Based on this definition we can determine a domain of accelerator tasks that can be potentially solved using ML techniques. Such tasks can be concerned by building models where analytical solutions do not exist, but the models can be “learned” from given examples instead of building them from sets of explicit rules. When building ML solutions, we should define a performance measure, e.g. accelerator performance parameter such as beam size or pulse energy. It is also important to differentiate a specific “class of task”, such that ML tools are designed for particular accelerator components which can be easily tested and controlled. Currently existing ML-based methods for accelerators can be divided into virtual diagnostics, control and optimization, anomaly detection and predictive modeling. A more detailed overview for beam diagnostics can be found in [2, 3], recent advances for the field of ML for accelerators control are described in [4–7].

Most of the ML efforts in accelerator physics are being developed for automatic machine optimization, since ML methods demonstrate notable advantages compared to numerical techniques in solving control tasks for non-linear, time-varying systems with large parameter spaces. Two techniques have found an especially wide application in this domain - Bayesian optimization [8] and Reinforcement Learning [9, 10]. Control tasks can be approached in both model-based and model-independent ways, e.g. using adaptive learning techniques to implement feedback algorithms for optimizing and tuning complex noisy systems [11–13]. Predictive modeling techniques also include Gaussian Processes, which can be used to build models relating a set of parameters (e.g. quadrupole settings) to an optimization

<sup>\*</sup> elena.fol@cern.ch

# A NOVEL NONDESTRUCTIVE DIAGNOSTIC METHOD FOR MeV ULTRAFAST ELECTRON DIFFRACTION

X. Yang<sup>†</sup>, J. Li, M. Fedurin, V. Smaluk, L. Yu, L. Wu, Y. Zhu, T. Shaftan,  
Brookhaven National Laboratory, Upton, NY 11973, USA  
W. Wan, ShanghaiTech University, Shanghai, China

## Abstract

A real-time non-destructive technique to monitor Bragg-diffracted electron beam energy, energy-spread, and spatial-pointing jitter by analysis of the mega-electron-volt ultrafast electron diffraction pattern, is experimentally verified. The shot-to-shot fluctuation of the diffraction pattern is decomposed into two basic modes, i.e., the distance between the Bragg peaks as well as its variation (radial mode) and the overall lateral shift of the whole pattern (drift mode). Since these two modes are completely decoupled, the Bragg-diffraction method can simultaneously measure the shot-to-shot energy fluctuation with  $2 \cdot 10^{-4}$  precision and spatial-pointing jitter in the wide range from  $10^{-4}$  to  $10^{-1}$ . The key advantage of this method is the possibility to extract the electron beam energy spread concurrently with the ongoing experiment. This enables the online optimization of the electron beam, especially for future high-charge single-shot ultrafast electron diffraction (UED) and ultrafast electron microscopy (UEM) experiments. Furthermore, the real-time energy measurement enables filtering out off-energy shots, improving the resolution of time-resolved UED. As a result, this method can be applied to the entire UED user community, beyond the traditional electron beam diagnostics used by accelerator physicists.

## INTRODUCTION

In recent years, there has been a growing interest in developing single-shot mega-electron-volt (MeV) ultra-fast electron diffraction (UED) systems [1-12]. Comparing to the commonly used electron diffraction in the 100 keV energy range, the main advantages of relativistic electron diffraction are reduced space charge effects and the higher penetration depth. The UED can also resolve much finer structural details compared to X-rays due to the hundreds-fold shorter wavelength of electrons in the required sub-picosecond timescale. However, single-shot imaging with high spatial resolution and small beam size on the sample is a significant challenge and it requires much brighter electron sources. For instance, the RF gun needs to be three orders of magnitude brighter than the present state-of-the-art guns to outrun beam-induced damage of the sample in biomolecular single-particle imaging, achieving “diffraction-before-destruction” [13]. On the other hand, the multi-shot operation requires significantly reduced beam brightness, but with much lower tolerances to the shot-to-shot energy and spatial-pointing fluctuation. To meet these requirements, we need a real-time non-destructive monitor

of the electron beam energy and spatial-pointing jitter to characterize the shot-to-shot energy fluctuation and energy spread of the electron beam.

Here we report our proof-of-principle experiment of characterizing the shot-to-shot energy jitter, spatial-pointing jitter, and energy spread of the electron beam for UED and UEM using a novel Bragg-diffraction method (BDM). The experiment was carried out on the existing high-charge high-brightness low-energy electron source developed at Brookhaven National Laboratory (BNL) with the capability of generating 3.3 MeV electron bunches with 10 pC charge ( $0.62 \cdot 10^8$  electrons) and 0.1 to 1 ps bunch length [10,11]. We were able to measure simultaneously the shot-to-shot energy fluctuation and spatial-pointing jitter of the electron beam in real-time via eigen-decomposing the variation of the diffraction pattern to two decoupled modes (radial and transverse) and obtain the dispersion of the beamline optics at the detector. Beyond tracking changes of the intensity, position, and width of diffraction patterns [14], we applied the dispersion and Bragg-diffraction (BD) peak width to extract the beam energy spread. The measured beam energy spread agrees reasonably well with Impact-T simulations [15] and with the direct beam-size measurement without crystal diffraction. The non-destructive measurement of the electron beam parameters and beamline optics opens a possibility of online minimization of the shot-to-shot energy jitter, spatial-pointing jitter, and energy spread, which is impossible with the conventional dipole-based diagnostic tools. We have experimentally demonstrated the BDM can provide a nearly complete set of beam-based diagnostic information for online optimization of the RF system stability and minimization of the dispersion at the detector. This is crucial for the future development of single-shot UED and UEM facilities with high-charge electron beam.

## EXPERIMENTAL RESULTS

The schematic layout of the UED setup is shown in Figure 1a. The peaks of a BD image shown in Fig. 1b are formed by the summation of the intensity distribution of all diffracted electrons. The diffraction pattern of a single electron is determined by the constructive interference governed by Bragg's law  $2d \sin \theta = n\lambda$ , where  $\theta$  is the incident angle,  $d$  is the crystal interplanar distance,  $\lambda$  is the de Broglie wavelength,  $n$  is the order of Bragg reflections. For the data analysis, we choose two BD peaks ( $i$  and  $j$  in Fig. 1b) with the largest separation, highest peak intensities, the same reflection order ( $n_{i,j} = n$ ) and crystal interplanar distance ( $d_{i,j} = d$ ). Before, we compared the result

<sup>†</sup>xiyang@bnl.gov

# FLASH RADIATION THERAPY: ACCELERATOR ASPECTS

Patriarca<sup>†</sup>, L. De Marzi, S. Meyroneinc, V. Favaudon, Institut Curie, Orsay, France

## Abstract

One of the new paradigms in radiation therapy (RT) is the FLASH dose delivery irradiation technique. The FLASH methodology consists in delivering millisecond pulses of radiation (total beam-on time < 100-500 ms) delivered at a high mean dose-rate (> 40-100 Gy/s) and pulse amplitude ( $\geq 106$  Gy/s), over 2000 times faster than in conventional RT. New accelerator ideas are under development or are being tested to deliver this type of beam. In this paper we will report the accelerator technology used for the pre-clinical studies and the necessary developments to deliver this novel dose RT technique.

## INTRODUCTION

Radiation therapy (RT) is one of the most effective cancer treatment and control, and is used in the treatment of 50 to 60% of cancers. Over 95% of the cancer treatment using RT techniques are realised with linear accelerators delivering MV photons or electron of less than 25 MeV. These machines are combined with multi-leaf collimators to adapt the beam to the tumour shape and imaging devices for positioning the patient. One of the main limitations of RT is that the dose delivered to the tumour is constrained by the dose that can be tolerated by the surrounding normal tissues. Recently, a strategy to overcome this limitation, based on the optimisation of the dose delivery method by using non-conventional temporal microstructures of the beam was proposed [1]. The so-called FLASH-RT has emerged. In the following, a short review of the main pre-clinical radiobiology studies is presented with a special focus on the accelerators used to deliver a FLASH irradiation. Subsequently the up-to-date machine designs for clinical applications are discussed.

## THE FLASH EFFECT

The "FLASH effect" was proposed by Favaudon et al. at Institut Curie (France) [1] as the result of very high dose-rate irradiation (pulse amplitude  $\geq 10^6$  Gy/s, or mean dose rate > 40 Gy/s), short beam-on duration ( $\leq 500$  ms) and large doses per fraction ( $\geq 10$  Gy) on in-vivo samples [2]. The lung fibrogenesis in C57BL/6J mice receiving 15–17 Gy in bilateral thorax irradiation with 4.5 MeV pulsed electron beams was investigated. Animals were exposed to single doses in short pulses so that the total irradiation time was less than 500 ms. Mice were also exposed to "conventional" (CONV) dose-rate irradiations ( $\leq 0.03$  Gy/s). No complications were developed on the healthy tissues after a FLASH irradiation (up to 23 Gy), while the CONV treatment generates lung fibrosis in the totality of the irradiated animals. In contrast, FLASH was as efficient as CONV when irradiating tumours (Fig. 1).

<sup>†</sup> annalisa.patriarca@curie.fr

These results were also reproduced and thoroughly extended by several teams in the last five years. In particular, the group headed by Dr. Vozenin in Lausanne (Switzerland) reported excellent results on mice, cats, pigs (summarised in a review article [3]), and a promising outcome in the treatment of a first human patient has also been reported [4]. Very recently, the biological mechanisms that underlie the FLASH effect in lung have also been identified [5].

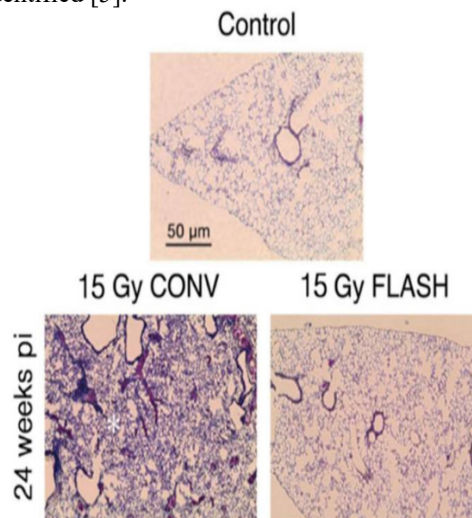


Figure 1: FLASH irradiation spares lung at doses known to induce fibrosis in mice following conventional dose-rate irradiation (CONV) (modified from [1]).

## ACCELERATORS USED IN THE PRE-CLINICAL FLASH STUDIES

In the next section, an overview of the machines used to study the FLASH effect is presented.

### Prototypes Low-Energy Electron LINACs

**Kinetron**, the "reference" accelerator used by Dr. Favaudon at Institut Curie is a S-band linear electron accelerator designed by a French company (CGR-MeV) in 1987 to investigate free radical reactions in macromolecules at the submicrosecond time-scale and the electron transfer kinetics [6] (Fig. 2). It is a compact electron linac with nominal energy of 4.5 MeV, and a set of parameter easily adjustable as the pulse repetition frequency (0.1 – 200 Hz), the pulse length (0.05 – 2  $\mu$ s) and with a mean dose rate up to 7000 Gy/s. The Kinetron is powered by a magnetron and is fitted with a thermionic triode electron gun. Precise adjustment of the grid potential of the triode allows the total control of the emitted current and pulse width in the FLASH operating mode. A more complete description of the machine parameters can be found in [6, 7].

**Oriatron eRT6**, the general design of the machine by PMB-Alcen was derived by the Kinetron. The 6 MeV



# CERN-MEDICIS: A UNIQUE FACILITY FOR THE PRODUCTION OF NON-CONVENTIONAL RADIONUCLIDES FOR THE MEDICAL RESEARCH

C. Duchemin<sup>1,2</sup>, J. P. Ramos<sup>1,2,\*</sup>, T. Stora<sup>1,†</sup>, E. Aubert<sup>1</sup>, N. Audouin<sup>3</sup>, E. Barbero<sup>1</sup>, V. Barozier<sup>1</sup>, A. P. Bernardes<sup>1</sup>, P. Bertreix<sup>1</sup>, A. Boscher<sup>1</sup>, D. Burnel<sup>1</sup>, R. Catherall<sup>1</sup>, M. Cirilli<sup>1</sup>, E. Chevallay<sup>1</sup>, T. E. Cocolios<sup>2</sup>, J. Comte<sup>1</sup>, B. Crepieux<sup>1</sup>, M. Deschamps<sup>1</sup>, K. Dockx<sup>2</sup>, A. Dorsival<sup>1</sup>, V. N. Fedosseev<sup>1</sup>, P. Fernier<sup>1</sup>, R. Formento-Cavaier<sup>1,3</sup>, V. M. Gadelshin<sup>1,4,5</sup>, S. Gilardon<sup>1</sup>, J. L. Grenard<sup>1</sup>, F. Haddad<sup>3,6</sup>, R. Heinke<sup>2</sup>, B. Jui<sup>1</sup>, M. Khan<sup>7</sup>, U. Köster<sup>8</sup>, L. Lambert<sup>1</sup>, G. Lilli<sup>1</sup>, G. Lunghi<sup>1</sup>, B. A. Marsh<sup>1</sup>, Y. Martinez Palenzuela<sup>2</sup>, R. Martins<sup>1</sup>, S. Marzari<sup>1</sup>, N. Mena<sup>1</sup>, N. Michel<sup>3,6</sup>, F. Pozzi<sup>1</sup>, F. Riccardi<sup>1</sup>, J. Riebert<sup>1</sup>, N. Riggaz<sup>1</sup>, S. Rothe<sup>1</sup>, S. Stegemann<sup>2</sup>, Z. Talip<sup>9</sup>, J. Thiboud<sup>1</sup>, N. P. van der Meulen<sup>9</sup>, J. Vollaire<sup>1</sup>, N. T. Vuong<sup>1</sup>, K. Wendt<sup>4</sup>, S. Wilkins<sup>1</sup>,  
on behalf of the CERN-MEDICIS collaboration

<sup>1</sup>CERN, Geneva, Switzerland

<sup>2</sup>KU Leuven, Institute for nuclear and radiation physics, Leuven, Belgium

<sup>3</sup>GIP ARRONAX, Nantes, France

<sup>4</sup>Johannes Gutenberg University, Mainz, Germany

<sup>5</sup>Ural Federal University, Yekaterinburg, Russia

<sup>6</sup>SUBATECH, Institut Mines Telecom Atlantique, CNRS/IN2P3, Université de Nantes, France

<sup>7</sup>Pakistan Institute of Nuclear Science and Technology, Islamabad, Pakistan

<sup>8</sup>Institut Laue Langevin, Grenoble, France

<sup>9</sup>Paul Scherrer Institute, Villigen, Switzerland

## Abstract

CERN-MEDICIS (MEDical Isotopes Collected from ISolde) is a facility at CERN (Switzerland) dedicated to the production of non-conventional radionuclides for research and development in imaging, diagnostics and radiation therapy done at partner institutes. It exploits, in a controlled radiation area suited for the handling of unsealed radioactive sources, a target irradiation station positioned between the High Resolution Separator (HRS) ISOLDE target station and its beam dump, a target remote handling system and a dedicated isotope separator beam line. It irradiates targets with the 1.4 GeV Proton Synchrotron Booster (PSB), and also receives activated target materials from external institutes, notably during CERN's Long Shut-Downs. The irradiated target is heated to high temperatures (up to 2300°C) to allow for the release of the isotopes of interest out of the target which are subsequently ionized. The ions are accelerated and the beam is steered through an offline mass separator. The radionuclide batches are, this way, extracted through mass separation and implanted into a thin metallic collection foil up to an energy of 60 keV. After collection, the isotope source is prepared to be dispatched to biomedical research centers (Figure 1).

Since its commissioning in December 2017, the CERN-MEDICIS facility has provided non-conventional medical radionuclides such as Tb-149, Tb-152, Tb-155, Tm-165, Er-169 and Yb-175 with high specific activity, some for the first time, to research institutes and hospitals, being part of the MEDICIS collaboration, for R&D in imaging or treatment [1].

\* Current affiliation: SCK CEN, Mol, Belgium

† Corresponding author: thiery.stora@cern.ch

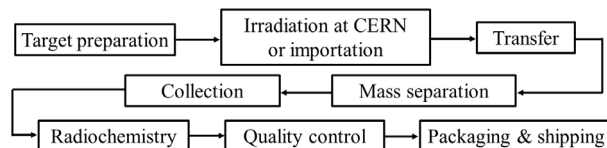


Figure 1: CERN-MEDICIS' steps from target preparation to radioisotopes shipping.

## THE CERN-MEDICIS COLLABORATION

The research program at CERN-MEDICIS is driven by a collaboration agreement between CERN and several partners which includes research institutes, hospitals and universities [1]. The installation has been built as an extension of the ISOLDE facility [2] for research purposes on medical isotopes in view of providing the collaborating institutes with radioisotopes of high specific activity for their research programs [3]. The CERN-MEDICIS scientific program is shaped from the biomedical projects submitted by the members to the Collaboration Board which evaluates the needs of the community and the technical feasibility. The first collection of radionuclides took place in December 2017 at the end of the commissioning period. Since then, the collaboration board approved already 25 proposals. The list of radionuclides of interest once defined is thus re-evaluated at each board, mostly for applications in theranostics, combining diagnosis and therapy. Among them we can find scandium isotopes such as Sc-44 and Sc-47 [4-6]. Sc-44 is of interest for Positron Emission Tomography (PET) and Sc-47 for use in both, therapy and Single Photon Emission Computed Tomography (SPECT). As for Sc-47, Cu-67 is a radionuclide of interest for theranostic

# DEVELOPMENT OF A HYBRID ELECTRON ACCELERATOR SYSTEM FOR THE TREATMENT OF MARINE DIESEL EXHAUST GASES\*

T. Torims<sup>†</sup>, G. Pikurs, K. Kravalis, A. Ruse, Riga Technical University, Riga, Latvia  
A. G. Chmielewski, A. Pawelec, Z. Zimek  
Institute of Nuclear Chemistry and Technology, Warsaw, Poland  
G. Mattausc, Fraunhofer Institute for Organic Electronics,  
Electron Beam and Plasma Technology FEP, Dresden, Germany  
M. Vretenar, CERN, Geneva, Switzerland

## Abstract

The paper outlines the overall results of the ARIES Proof-of-Concept (PoC) project,<sup>1</sup> which seeks to tackle the shipping industry's most pressing problem, its large-scale emissions of nitrogen oxides (NO<sub>x</sub>), sulphur oxides (SO<sub>x</sub>) and particulate matter (PM), by developing a hybrid exhaust gas-cleaning technology that combines an EB accelerator with improved wet-scrubbing technology. It is unique – in a single technological system – and addresses all three types of emissions simultaneously. It promises to be cheaper and more efficient than existing solutions. There are two main stages involved: 1) SO<sub>2</sub> and NO<sub>x</sub> oxidation during the irradiation of wet gases by the EB from the accelerator and 2) the absorption of pollution products into an aqueous solution. For the very first time, test trials in a real maritime environment were conducted and attracted the interest of the maritime industry, policy makers and the accelerator community. The PoC has clearly confirmed the potential of this technology and forms a solid basis for the full-scale application of the hybrid system on sea-going ships. The results of this project are of the highest relevance to the accelerator community, as well as the maritime industry and policy makers.

## MOTIVATION AND CONTEXT

Heavy fuel oil (HFO) is the main energy source used by the maritime industry. Almost all medium and low-speed marine diesel engines run on HFO with a high sulphur content, leading to the formation of three main pollutants: NO<sub>x</sub>, SO<sub>x</sub> and PM. These emissions have been gradually restricted worldwide. When entering Emission Control Areas (ECA) or ports, ships switch to 0.1% sulphur content fuel, marine gasoil (MGO). Since 2020, maritime transport has had to comply with the worldwide 0.5% emission sulphur cap, under MARPOL Annex VI Regulation 14.

In the North America ECA, not only SO<sub>x</sub>, but also NO<sub>x</sub> and PM have been regulated and the North/Baltic Sea Sulphur ECA will be in place from 2021. A similar policy initiative is currently undertaken in the Mediterranean Sea [1]. These are so-called Tier III requirements, limiting NO<sub>x</sub> emissions to between 3.4 and 2 g/kWh. It is expected that further requirements for significant PM reductions will

be imposed [2]. The maritime community faces a serious challenge to fulfil these limitations [3].

## Existing Technologies and Prior Attempts

**Cutting SO<sub>x</sub>.** To comply with sulphur emission limitations [4], the shipping industry currently has two workable options [5]: a) to opt for universal usage of expensive MGO, or b) to install exhaust gas cleaning systems (scrubbers [6]), which reduce SO<sub>x</sub> and PM emissions from ship engines, generators and boilers, allowing ships to continue using HFO.

However, there may be pertinent operational issues involved in running marine engines designed for HFO continuously on MGO and the price difference between the two could considerably increase shipping costs. Today scrubbers are the preferred solution to comply with SO<sub>x</sub> limitations, hence there is a growing incentive for ship owners to invest in scrubbers. However, implementation costs are very high: 1M to 5M EUR for the equipment [7] alone. Therefore, in the absence of a more cost-effective technological solution, it will be very challenging in the near future to equip the global fleet of about 60,000 vessels.

**Dealing with NO<sub>x</sub>.** NO<sub>x</sub> production is not directly related to the type of fuel, but to the combustion process itself. Switching to MGO therefore doesn't solve this issue. In order to achieve NO<sub>x</sub> emission compliance, some form of additional technology has to be installed on-board. Usually this is a costly and complicated, selective catalytic reduction (SCR) system. Naturally, marine scrubbing and denitration systems are expected to be compatible, although this is not the case. As such, ships are being equipped with two separate purifying systems: one for SO<sub>x</sub> and another for NO<sub>x</sub>.

**PM trapping.** The most common methods for removing PM from exhaust fumes are the Continuously Regenerating Trap, Diesel Particulate Filter and Diesel Oxidation Catalyst. However, they can only be used for emissions from low-sulphur fuels. Also the nanoparticles, the most harmful form of PM (e.g. PM<sub>10</sub> and PM<sub>2.5</sub>) are not sufficiently prevented from entering the ambient air.

**Prior attempts.** The ship-emission challenge is not new *per se*; there have been various efforts to find feasible alternatives, such as the Humid Air Motor, Exhaust Gas Recirculation, Plasma-Catalysis, Nano-Membrane Filters, etc. Several of these projects [8-12] were EU financed and presented to the stakeholders. Yet to this day, they cannot

\* This project has received funding from the European Union's Horizon 2020 Research and Innovation programme under grant agreement No 730871

<sup>†</sup> toms.torims@rtu.lv

# ACCELERATORS FOR APPLICATIONS IN ENERGY AND NUCLEAR WASTE TRANSMUTATION

A. Fabich†, D. Vandeplassche, U. Dorda, H. Ait Abderrahim, SCK CEN, Mol, Belgium

## Abstract

SCK CEN is at the forefront of Heavy Liquid Metal (HLM) nuclear technology worldwide with the development of the MYRRHA accelerator driven system (ADS) [1]. An Accelerator Driven System (ADS) is a concept using high power proton accelerators in energy production and nuclear waste transmutation. Amongst typical beam performance requirements, the operational reliability of the accelerator is exceptionally demanding. The advantages and challenges of different driver options, like cyclotrons and linacs, are evaluated and worldwide design studies are summarized. The MYRRHA design is based on a 600 MeV superconducting proton linac. The first stage towards its realization was recently approved to be constructed by SCK CEN in Belgium. The 100 MeV linac will serve as technology demonstrator for MYRRHA as well as driver for two independent target stations, one for radioisotope research and production of radio-isotopes for medical purposes, the other one for fusion materials research. MYRRHA in its final implementation is envisaged as an international large research infrastructure open for scientific and industrial user-communities.

## MOTIVATION FOR ADS

While alternative, renewable energy sources combined with increased efficiencies are being developed, there remains the clear need for complementary large-scale base-load power stations and a strategy for handling the already accumulated nuclear waste. Conventional reactors feature the following two main issues:

- Operation of a critical system: The neutrons emitted during the fission of one atom hit other atoms and trigger their fission. In order to keep the system running, a multiplication factor of  $K = 1$  must be used. This factor is defined by the fission material and reactor configuration. The only control is given by the insertion of additional absorbing elements that limit the exponential increase of activity.
- Radiotoxic waste with  $>10,000$  years half life time. The minor actinides (Np, Am, Cm) are the main concern due to their high radiotoxicity, heat emission and long half-life.

The concept of an ADS [2] is to load the reactor with subcritical mass of fissile material ( $k_{eff} < 1$ ). Left alone, this implies that the chain reaction would naturally shut down exponentially with time (in the order of  $10^{-5}$  to  $10^{-6}$  sec). In order to keep the chain reaction going and hence the power level constant in the reactor, additional neutrons are provided from a spallation target inside the reactor that is driven by a high-power proton particle accelerator. In case

of issues, the accelerator is turned off and the chain reaction automatically slows down. This also removes the need for highly enriched fission material.

These kinds of reactor will be loaded with the Plutonium and Minor Actinides “waste” resulting from the reprocessed spent fuel of the nuclear power plants. With help of the subcritical reactor, transmutation can be efficiently achieved. In contrast to conventional reactors, an ADS can safely transmute a large amount of these minor actinides. As shown in Fig. 1, an ADS allows to reduce the time needed to store the nuclear waste to a level that is compatible with the lifetime of human-made buildings.

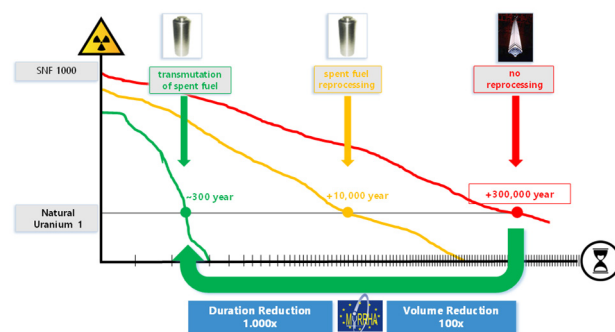


Figure 1: While reprocessing of waste and reuse of Pu in conventional reactors allows to reduce the burden of nuclear waste radiotoxicity by a factor 30, an ADS can reduce the life time by a factor 1000.

## REQUIREMENTS ON THE ACCELERATOR

While the exact requirements on the particle accelerator will depend on the design details of the reactor, the following beam requirements can be stated:

- Particle type: protons, readily available and accelerated for neutron production
- Energy:  $>500$  MeV to be in the region of usable neutron production cross-section.
- Beam power: multiple MW, achieving a usable neutron density.
- Reliability: MTBF  $>$  multiple weeks. Any beam trips must be resolved within a few seconds as otherwise this would impose severe thermal stress on the reactor materials and components. Furthermore, any longer beam trip requires a time-consuming reactor restart lasting a few days.
- The beam emittances are only important to safely accelerate and transport the beam through the accelerator.

From this list the following additional design choices can be derived:

† Adrian.fabich@sckcen.be